*Journal of Applied Electrochemistry* **31**: 1293–1300, 2001.



# Kinetics of molecular oxygen electroreduction on platinum modified by tin underpotential deposition

C.F. ZINOLA*, J. RODRÍGUEZ and G. OBAL
*Laboratorio de Electroquímica Fundamental, Facultad de Ciencias, Universidad de la República, Avda. Libertad No. 2497, C.P. 11300, Montevideo, Uruguay*
*(*Author for correspondence)*

Received 14 August 2000; accepted in revised form 12 June 2001

*Key words:* oxygen electroreduction, platinum, ring-disc techniques, tin, underpotential deposition

**Abstract**

The kinetics of molecular oxygen electroreduction were studied on platinum surfaces modified by tin underpotential deposition. The surface process was analysed by cyclic voltammetry in aqueous $10^{-4}$ M tin(II)/1 M sulfuric acid in the 0.05 to 0.70 V vs RHE range. Platinum sites involving (1 1 0) planes are mainly related to tin underpotential deposition as observed in the hydrogen sorption region. Kinetic runs for oxygen reduction were performed with the rotating ring-disc electrode technique on tin-modified platinum surfaces. It was concluded that molecular oxygen reduction on tin-modified platinum takes place through bulk hydrogen peroxide and water formation. This interpretation was confirmed by calculating the reaction order with respect to oxygen. Electrochemical rate constants for oxygen reduction pathways were calculated as a function of deposition potential based on Damjanović's reaction scheme.

## 1. Introduction

Fuel cell performance is mainly limited by the high overpotential involved in the oxygen electroreduction reaction (OERR) [1, 2]. This reaction rate can be increased by using alternative electrolytes or by making an appropriate change in the electrode surface composition [3, 4], for instance by underpotential deposition (UPD) of different metals at sub- or monolayer levels [5, 6]. Copper UPD has been extensively studied on platinum in acid media [7, 8], and the OERR kinetics showed a strong inhibition of the four-electron pathway in favour of the two-electron path [9].

Two Tafel regions have been found for the OERR on polycrystalline (pc) platinum in aqueous acid solutions, namely, $-0.060$ V decade$^{-1}$ and $-0.120$ V decade$^{-1}$ in the low and high cathodic overpotential ranges, respectively [10, 11]. This reaction can be explained by a mechanism involving two parallel processes [11–13]. The first consists of a direct four-electron transfer reduction of molecular oxygen to water and the second involves a two-electron transfer reduction leading to hydrogen peroxide, which is either electroreduced to water or diffused to the bulk. The relative contribution of each pathway to the net reaction depends on experimental conditions [1–4, 10–13]. Moreover, a crystallographic influence of platinum electrodes on hydrogen peroxide formation has been reported in different electrolytes [10, 11].

The low oxidation potential of tin makes it an interesting material to enhance catalytic oxidation processes [14–17]. Several papers have discussed tin UPD on platinum [15–20], however, overlapping UPD and bulk processes yield contradictory results in certain conditions. It has been found [21, 22] that the adsorption of a tin monolayer from tin(II) species in aqueous hydrochloric acid produced unstable films on gold. On the other hand, it has been shown using Mössbauer spectroscopy [22] that there is no difference between tin UPD and bulk deposition processes. In the late nineties, tin UPD species on Pt(3 3 2) and Pt(7 5 5) single crystals were analysed as possible substitutes for hydrogen-adatoms [19, 20]. Catalytic effects of tin-adatoms have also been advanced [16, 17] for formic acid and carbon monoxide oxidations on pc platinum surfaces.

For any UPD process, Cadle and Brückenstein [23] found a preferred occupation site by the foreign metal, when atomic radii of this metal (tin) and that of the substrate (platinum) are similar. The result is the inhibition of a particular type of platinum–hydrogen interaction. However, Motoo and Furuya [24] postulated a rearrangement for copper UPD on platinum from disordered to ordered surface structures with the simultaneous appearance of free platinum sites, even for more than one monolayer.

The aim of this work is to gain insight into the influence of tin UPD on the OERR kinetics at pc platinum in aqueous sulfuric acid solutions and to envisage the

possibility of changing platinum catalytic properties for the UPD of an easily oxidized metal such as tin.

## 2. Experimental details

Mirror-polished pc platinum disc working electrodes were prepared using alumina pastes of different grades, subsequently immersed in a 1:1 pure nitric–sulfuric acid mixture for 1 h, and then, repeatedly rinsed with Millipore-MilliQ* water. The platinum real surface area was estimated from the voltammetric hydrogen-adatom charge at 0.10 V $s^{-1}$ after double-layer correction [25]. A large-area platinum plate counter electrode (50 $cm^2$ in geometric area) facing the disc electrode and a reversible hydrogen reference electrode (RHE) in the same electrolyte were employed. All potentials in the text are given on the RHE scale and all experiments were performed at 25 °C. Purified sulfuric acid (Merck, 98.6% 'for Synthesis'), tin(II) nitrate (Sigma) and Millipore-MilliQ* water were used to prepare working solutions. Before each electrochemical measurement, the cleanness of the system was checked by cyclic voltammograms run at 0.10 V $s^{-1}$ in the 0.05–1.50 V range. Using the entire treatment given above for pc platinum, negligible voltammetric changes were found after potential holding at 0.60 V for 10 min.

Tin UPD deposition was performed using the following procedure:

(i) First, the stable cyclic voltammogram of pc platinum disc was obtained in aqueous 1 M sulfuric acid (supporting electrolyte) by repetitive cycling between 0.05 and 1.50 V.
(ii) Secondly, the electrolyte was replaced by the tin(II)-containing supporting electrolyte and a fixed potential applied within the 0.05–0.70 V range for 5 min.
(iii) Finally, the electrolyte was replaced again by supporting electrolyte and the electrode potential cycled in the hydrogen sorption region to obtain a stable tin surface coverage ($\theta_{Sn}$). The values of $\theta_{Sn}$ were evaluated as explained in Section 3.1.

Three variables were taken into account to control tin UPD process: tin(II) concentration, deposition time and applied potential. The results were obtained at a fixed $10^{-4}$ M tin(II) concentration.

Kinetic runs were conducted using the rotating ring-disc electrode technique in oxygen-saturated (99.99% purity AGA) supporting electrolyte with and without hydrogen peroxide (1 mM). The disc potential ($E_D$) was scanned from 1.0 to 0.05 V at 0.01 V $s^{-1}$ and the ring potential ($E_R$) was held at 1.20 V to electrooxidize hydrogen peroxide produced on the disc under a mass-transport regime. Values of disc ($I_D$) and ring ($I_R$) currents were recorded at different rotation speeds ($\omega$) in the 500 to 4000 rpm range. The collection efficiency of the ring-disc device was $N = 0.22$. The value of $N$ was checked with the $Fe(CN)_6^{3-}/Fe(CN)_6^{4-}$ redox couple in dilute alkaline media. Since kinetic experiments involved potentials greater than ~0.8 V; $\theta_{Sn}$ values were controlled between each run to obtain the real surface coverage value. However, when $\theta_{Sn}$ was larger than 0.1, a decrease by only 10% was observed.

## 3. Results and interpretation

### 3.1. *Cyclic voltammograms of tin UPD on pc platinum in sulfuric acid*

The tin electrodeposition potential was varied in 0.05 V steps from 0.70 to 0.05 V. Below 0 V rapid tin bulk deposition parallel with the hydrogen evolution reaction was observed in the supporting electrolyte, leading to irreversible bulk processes.

The first voltammetric profile of tin UPD on pc platinum in the supporting electrolyte does not exhibit a defined shape. Repetitive and reproducible current vs. potential profiles are obtained only after ten cycles between 0.05 and 0.60 V. It is interesting to observe the different and subsequent features during potentiodynamic cycling of tin UPD in this potential region (Figure 1). The anodic charge of peak II (involving (1 1 0) crystallographic sites) sharply diminishes, whereas that of peak III increases. This suggests that tin deposition is preferentially achieved on (1 1 0) sites and, consequently, some hydrogen species rearrange to (1 0 0) sites.

Steady state values of $\theta_{Sn}$ at any deposition potential can be calculated in two ways:

(i) From the ratio between voltammetric charges involved in the hydrogen sorption region before ($Q_H^0$) and after tin deposition ($Q_H$).

$$\vartheta_{Sn} = \frac{Q_H}{Q_H^\circ} \tag{1}$$

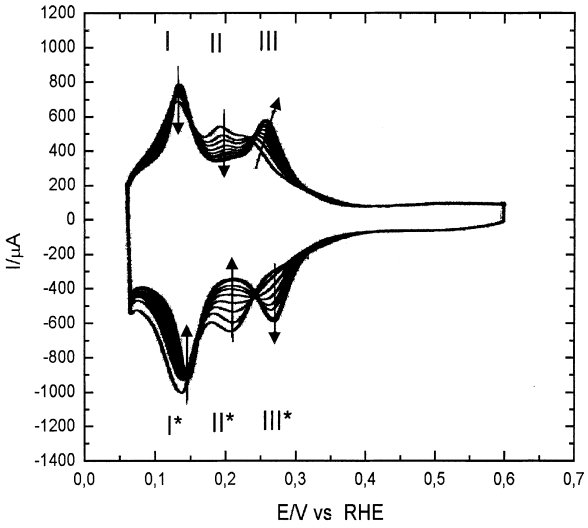


*Fig. 1.* Subsequent voltammetric cycles between 0.05 and 0.60 V for tin UPD ($\theta_{Sn} = 0.18$) on a pc platinum disc in supporting electrolyte. Real area 4.52 $cm^2$, $T = 25$ °C, $v = 0.10$ V $s^{-1}$. Arrows indicate cycling effects. Anodic peaks are labelled as I, II and III and cathodic peaks as I*, II* and III*.

(ii) From voltammetric charges observed in the tin anodic desorption profile, that is, from 0.35 to 1.1 V [26]. The number of platinum sites per tin atom and the number of electrons involved in the oxidation must be considered. According to literature data [18] a single tin atom requires two platinum atoms for UPD on pc surfaces, whereas an anodic desorption up to 1.1 V produces tin(II) species in solution [18]. Then, $\theta_{Sn}$ at any deposition potential is calculated by

$$\vartheta_{Sn} = \frac{Q_{Sn}}{2\,Q^{\circ}_{H}} \tag{2}$$

where $Q_{Sn}$ is the anodic desorption charge obtained from the current against potential profile.

The calculation of $\theta_{Sn}$ for tin UPD from Equations 1 and 2 yields equivalent values (±5%).

It seems that Furuya and Motoo's proposal [24] has been demonstrated for tin UPD on platinum, since the surface coverage by hydrogen adatoms plotted as a function of $1 - \theta_{Sn}$ yields a straight line. This also indicates that tin UPD inhibits further adsorption of hydrogen species. However, we have found a surface rearrangement by potentiodynamic cycling (Figure 1). Therefore, any further conclusions about the structure of tin layers on platinum have to be analysed in each experimental condition.

Figure 2 (points) shows steady state values of $\theta_{Sn}$ as a function of potential after 10 cycles (voltammetric stabilisation) in the 0.60–0.05 V range at 0.01 V $s^{-1}$. The isotherm exhibits a typical sygmoidal shape, that is, slowly increasing $\theta_{Sn}$ values between 0.70 and 0.45 V before reaching saturation ($\theta_{Sn} = 0.66$) from 0.25 to 0.05 V.

It is important to establish the type of isotherm by numerical fitting $\theta_{Sn}$ values. Since Temkin adsorption isotherms for tin UPD on platinum have already been observed [18], a similar isotherm was assayed and is depicted in Figure 2 (lines).

$$\left(\frac{\vartheta_{Sn}}{1-\vartheta_{Sn}}\right)\exp\left(\frac{r\vartheta_{Sn}}{RT}\right) = a_{Sn}^{2+}\exp\left(\frac{-\Delta G^{\circ}_{ad,\vartheta=0}}{RT}\right) \times \exp\left(\frac{-nFE}{RT}\right) \tag{3}$$

where $n = 2$ is the number of electrons involved in the UPD process, $a_{Sn}^{2+}$ is the activity referred to $10^{-4}$ M tin(II) concentration, $\Delta G^{\circ}_{ad,\theta=0}$ is the standard free energy of adsorption at zero surface coverage and the rest of the symbols have their usual meaning. By plotting $\ln(1-\theta_{Sn})/\theta_{Sn}$ against $\theta_{Sn}$ at each potential, we obtain $r$ (13 kJ $mol^{-1}$) from the slope and $\Delta_{ad,\theta=0}$ from the ordinate at $\theta = 0$ (−420 ± 40 kJ $mol^{-1}$). This value of $r$ covers the experimental error in $\Delta G^{\circ}_{ad,\theta=0}$ and does not change significantly (±10%) for increasing $\theta_{Sn}$ values.

### 3.2. *Rotating ring-disc voltammograms for the OERR on tin UPD pc platinum in sulfuric acid*

$I_D$ against $E_D$ and $I_R$ against $E_D$ rotating voltammograms were recorded for the OERR in oxygen-saturated supporting electrolyte (in the absence and presence of hydrogen peroxide) at pc platinum and tin UPD platinum (Figure 3). $E_D$ was scanned from 1.00 to 0.05 V at 0.01 V $s^{-1}$ at each selected $\omega$ (500, 1000, 2000, 3000 and 4000 rpm). However, in the case of hydrogen peroxide containing solutions, $E_D$ was scanned from 1.50 to 0.05 V at the same rate.

On the one hand, $I_D$ against $E_D$ and $I_R$ against $E_D$ voltammograms for OERR at bare platinum in oxygen-saturated supporting electrolyte are shown in Figure 3(a). Nonzero currents for the disc were obtained from 0.80 V downwards and the general contour exhibits the normal response of a mixed controlled reaction [10].

On the other hand, OERR at bare platinum in oxygen-saturated + 1 mM hydrogen peroxide (Figure 3(b)) exhibits nonzero currents from 1.50 V downwards due to

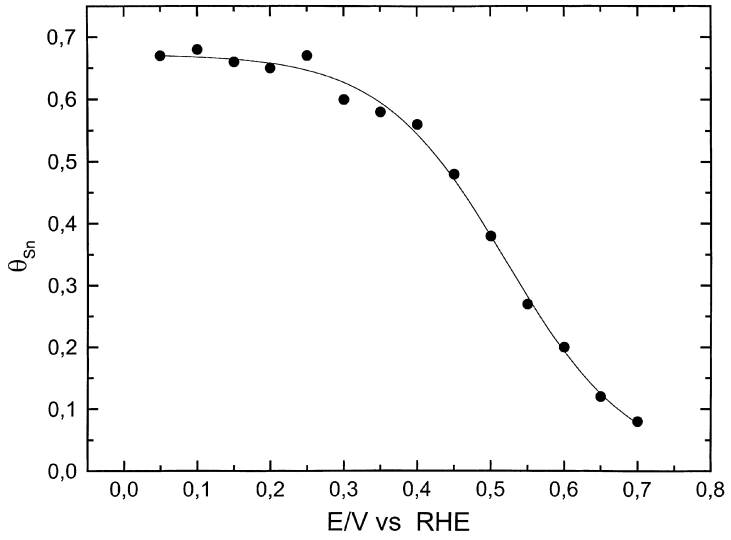


*Fig. 2.* $\theta_{Sn}$ against potential plot on pc platinum in supporting electrolyte at 25 °C. Charges involved in the process were voltammetrically calculated as described in the text. Each point results after voltammetric stabilization (10 cycles) in the 0.05–0.60 V range at $v = 0.10$ V $s^{-1}$.

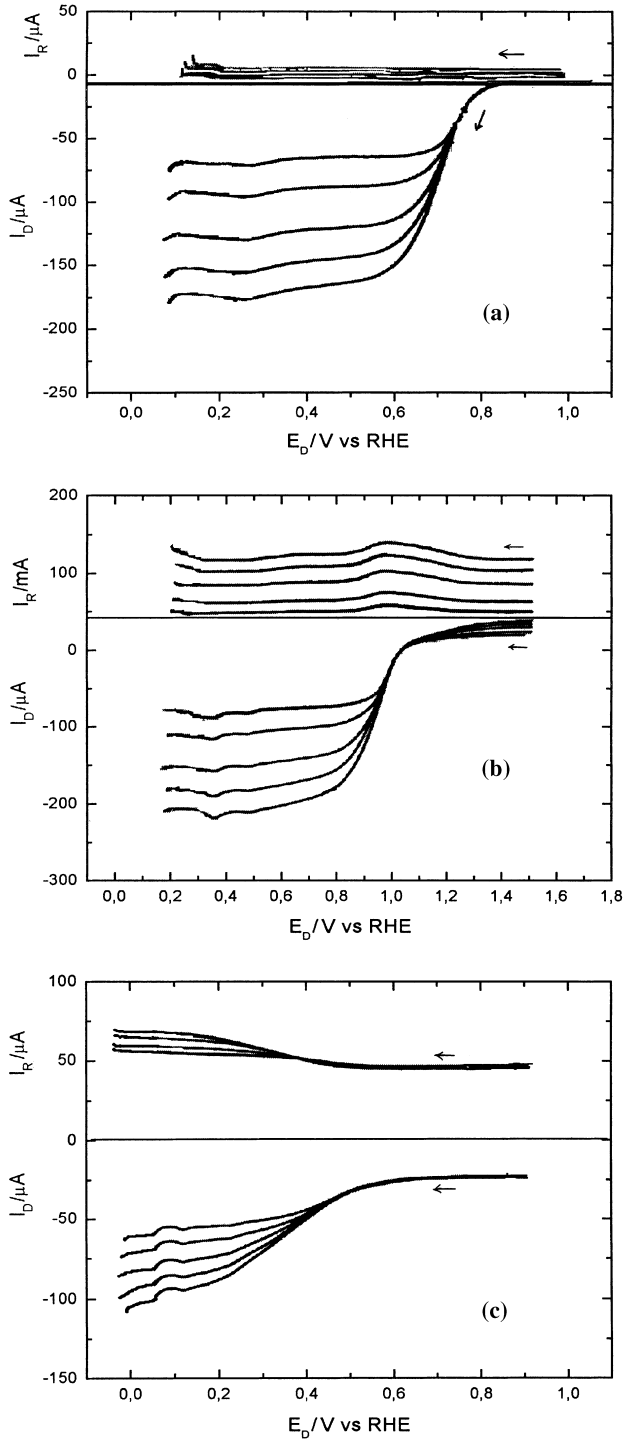


*Fig. 3.* Rotating $I_D$ against $E_D$ and $I_R$ against $E_D$ voltammograms recorded in (a) oxygen saturated supporting electrolyte at pc platinum; (b) oxygen saturated + 1 mM hydrogen peroxide supporting electrolyte at pc platinum; (c) oxygen saturated supporting electrolyte at tin UPD platinum ($\theta_{Sn} = 0.48$). $T = 25$ °C. $\omega = 500$, 1000, 2000, 3000 and 4000 rpm. $v = 0.010$ V s$^{-1}$. $E_R = 1.20$ V. Arrows indicate the scan direction.

hydrogen peroxide oxidation. Nevertheless, at potentials lower than 0.95 V, both hydrogen peroxide and oxygen reductions are observed. Two limiting currents are found as a consequence: one resulting from oxygen and hydrogen peroxide reductions and the other from hydrogen peroxide oxidation. Two contributions are observed in the $I_R$ against $E_D$ voltammogram: a background faradaic current due to hydrogen peroxide oxidation to oxygen and a current peak at ~0.9 V caused by peroxide adsorbates formation. Both effects increase with $\omega$ as expected for a mixed controlled reaction process. The $I_R$ peak coincides with the inflection point of the $I_D$ against $E_D$ voltammogram.

OERR kinetics at platinum surfaces modified by tin UPD have different characteristics. Therefore, Figure 3(c) shows OERR rotating voltammograms for $\theta_{Sn} = 0.48$ with two limiting currents, one due to oxygen electroreduction ($I_D$ against $E_D$) and another due to hydrogen peroxide oxidation ($I_R$ against $E_D$). It is important to emphasise that the existence of a limiting current on both voltammograms is an indication that OERR kinetics are not totally blocked by tin. As expected from the Levich equation both limiting currents vary linearly with the square root of $\omega$. Comparing these curves with those obtained for OERR at bare platinum, no peroxide adsorbates contributions in the $I_R$ against $E_D$ voltammogram are observed.

Results for OERR on tin UPD platinum differ from those found for copper UPD at platinum in acid media [9], since no further OERR inhibition by tin is observed below 0.20 V although free platinum active sites for OERR are always present because the saturation value of $\theta_{Sn}$ is not 1 but 2/3. However, $I_D$ values at each $\omega$ are almost one half of those obtained for OERR at bare platinum. This means that tin inhibits OERR by contributing to a greater hydrogen peroxide production.

### 3.3. *Reaction orders with respect to oxygen at tin UPD pc platinum in sulfuric acid*

The slopes of log ($I_D/I_k$) against log ($1 - I_D/I_{LD}$) plots can be used to evaluate the reaction order with respect to oxygen, $p$, at constant $E_D$. $I_k$ and $I_{LD}$ are kinetic and limiting diffusion disc currents, respectively. The value of $p$ found for OERR at pc platinum in supporting electrolyte was 0.5 ± 0.1 and 0.9 ± 0.1 at all $E_D$ values in the presence of 1 mM hydrogen peroxide. On the other hand, $p$ was 1.0 ± 0.1 independent of $\theta_{Sn}$ ($\theta_{Sn} > 0.05$) for OERR at tin UPD platinum. These values coincide with a reaction path involving the formation of peroxide adsorbates and bulk hydrogen peroxide, previously demonstrated by rotating ring-disc voltammograms. $p$ Values of ~1 have already been found for OERR on (1 0 0) preferentially oriented platinum in trifluoromethanesulphonic acid [11], whereas $p$ about 0.5 have been obtained for the same reaction on pc platinum in aqueous acid [12, 13].

## 4. Analysis of results and discussion

Among all reaction schemes, that proposed by Damjanović et al. [27] has been successfully applied to study OERR kinetics on platinum metals in aqueous solutions. It considers global series and parallel reaction

pathways comprising a direct oxygen electroreduction to water (path 1), a parallel electroreduction to hydrogen peroxide (path 2), and a further electroreduction of hydrogen peroxide to water (path 3). Each of these steps is characterised by electrochemical reaction rates, usually named $\bar{k}_1$, $\bar{k}_2$ and $\bar{k}_3$, respectively. Damjanović's mechanism can be presented as follows:

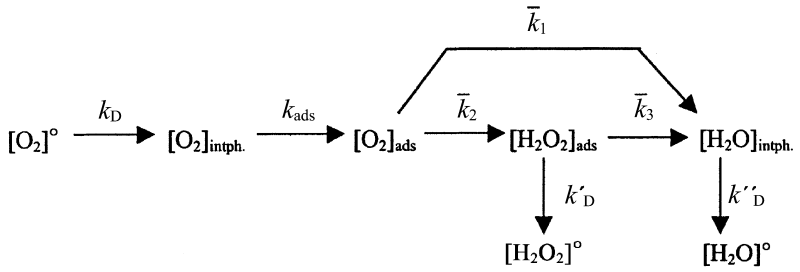


(I)

Mass transport rate constants for oxygen, hydrogen peroxide and water molecules diffusing to and from the surface, are named $k_D$, $k'_D$ and $k''_D$, respectively. Superscript $\circ$ stands for species located in bulk, whereas subscripts 'intph' and 'ads' stand for interphasial and adsorbed species, respectively.

Damjanović's scheme predicts the following relationships between $I_D$, $I_R$ and $I_{LD}$ with $\omega$:

$$\frac{I_{LD}}{I_{LD}-I_D} = 1 + \frac{\bar{k}_1+\bar{k}_2}{Z_1}\frac{1}{\sqrt{\omega}} \tag{4}$$

where $Z_1 \equiv 0.62\, D_{O_2}^{2/3} \nu^{-1/6}$.

$$\frac{I_D}{I_R} = \frac{1}{N}\left(1+\frac{2\bar{k}_1}{\bar{k}_2}\right) + \left[\frac{2\bar{k}_3\left(1+\bar{k}_1/\bar{k}_2\right)}{NZ_2}\right]\frac{1}{\sqrt{\omega}} \tag{5}$$

where $Z_2 \equiv 0.62\, D_{H_2O_2}^{2/3} \nu^{-1/6}$.

If this scheme is valid, Equation 4 will predict $I_{LD}/(I_{LD}-I_D) \to 1$ at $\omega^{-1/2} \to 0$. A linear behaviour in this plot suggests a negligible hydrogen peroxide chemical decomposition. Nevertheless, when the latter does not occur, Wroblowa's scheme has to be applied [1, 28].

Figures 4 and 5 show $I_D/I_R$ against $\omega^{-1/2}$ and $I_{LD}/(I_{LD}-I_D)$ against $\omega^{-1/2}$ plots for OERR in oxygen-saturated supporting electrolyte (in the presence and absence of hydrogen peroxide) at pc and tin UPD platinum. This type of analysis is usually not covered for OERR at bare pc platinum in acid solutions, since $I_R$ values are negligible.

Values of $S_1$ (slopes of $I_D/I_R$ against $\omega^{-1/2}$ plots) strongly depend on $E_D$ at bare platinum, whereas there is little influence of $S_1$ on $E_D$ in the presence of hydrogen peroxide. However, $I_1$ values (intercepts in $I_D/I_R$ against $\omega^{-1/2}$ plots) are large and dependent on potential for OERR at bare platinum, but small in the presence of hydrogen peroxide. As expected, at $E_D$ greater than 0.84 V, $I_1$ becomes $1/N \approx 3$–5. This shows the absence of a direct oxygen electroreduction due to the presence of surface oxides.

For OERR in the presence of hydrogen peroxide the situation is totally different. Thus, at $E_D$ lower than 0.68 V, a change in the sign of $S_1$ is observed due to the contribution of hydrogen peroxide oxidation (Figure 4(b)). By contrast, the behaviour of $I_D/I_R$ against $\omega^{-1/2}$ plots in the case of tin UPD is similar to that of hydrogen peroxide containing solutions for $E_D$ higher than 0.62 V. Values of $I_1$ independent of $E_D$ and small values of $S_1$ are observed (Figure 4 (c)).

Figure 5 shows that the intercept of the $I_{LD}/(I_{LD}-I_D)$ against $\omega^{-1/2}$ plot is exactly 1 for OERR at bare platinum and slightly greater than 1 ($\pm$20%) for the rest of the systems because of hydrogen peroxide production. The slopes of $I_{LD}/(I_{LD}-I_D)$ against $\omega^{-1/2}$ plots, $S_2$, are large and dependent on $E_D$ for OERR at bare platinum, whereas smaller values of $S_2$ are obtained with hydrogen peroxide within the 0.68–0.80 V range. In the case of tin UPD platinum, OERR defines $I_{LD}/(I_{LD}-I_D)$ against $\omega^{-1/2}$ plots similar to those of hydrogen peroxide containing solutions.

The following equations, resulting from Equations 4 and 5, offer $\bar{k}_i$ values at different $E_D$:

$$\bar{k}_1 = \frac{Z_1 S_2 (I_1 N - 1)}{(I_1 N + 1)} \tag{6}$$

$$\bar{k}_2 = \frac{2 Z_1 S_2}{(I_1 N + 1)} \tag{7}$$

$$\bar{k}_3 = \frac{N Z_2 S_1}{(I_1 N + 1)} \tag{8}$$

Table 1 depicts OERR rate constants on bare and tin UPD ($\theta_{Sn} = 0.48$) platinum. OERR at bare pc platinum exhibits the largest $\bar{k}_1$, which decreases monotonously with $E_D$. On the other hand, $\bar{k}_2$ and $\bar{k}_3$ are, in the same solution, respectively, 100 and 1000 times lower than $\bar{k}_1$ at all $E_D$, reaching maxima at 0.72 V. At $E_D$ greater than 0.80 V, $\bar{k}_1$ becomes nearly zero due to the catalytic formation of hydrogen peroxide at the oxidized platinum surface. On the other hand, the OERR rate constants obeyed at tin UPD ($\theta_{Sn} = 0.48$) platinum exhibit a different behaviour. $\bar{k}_1$ values are 10 times smaller than $\bar{k}_2$ and $\bar{k}_3$ and reach a maximum at 0.30 V.

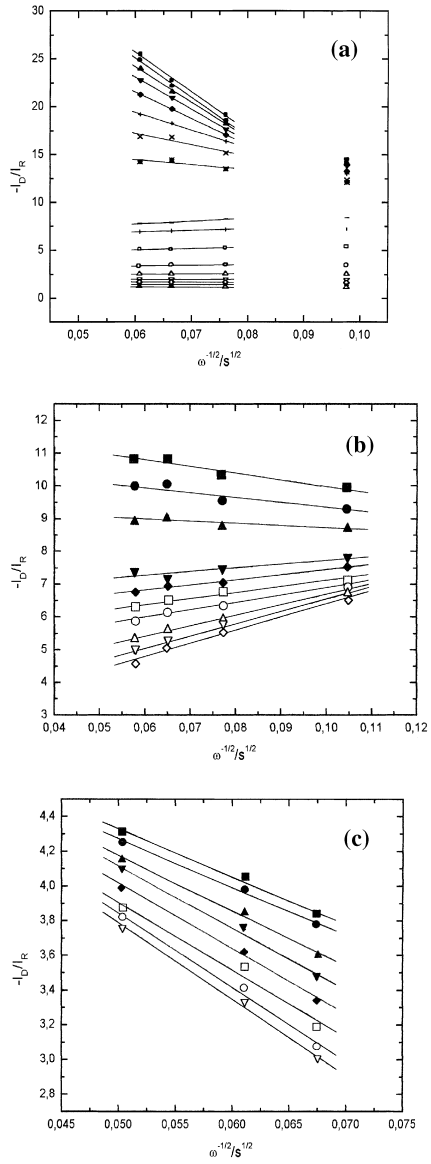


*Fig. 4.* $I_D/I_R$ against $\omega^{-1/2}$ plots in (a) oxygen saturated supporting electrolyte at pc platinum; (b) oxygen saturated + 1 mM hydrogen peroxide supporting electrolyte at pc platinum; (c) oxygen saturated supporting electrolyte at tin UPD platinum ($\theta_{Sn} = 0.48$). $T = 25$ °C. Key: (■—■) 0.60, (●—●) 0.62, (▲—▲) 0.64, (▼—▼) 0.66, (◆—◆) 0.68, (□—□) 0.80, (○—○) 0.82, (△—△) 0.84, (∇—∇) 0.86 and (◇—◇) 0.88 V.

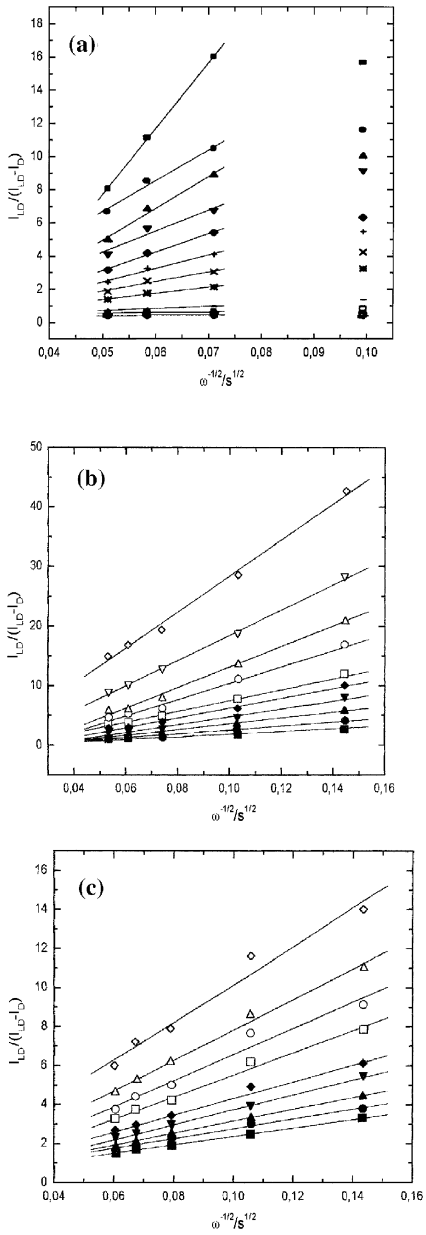


*Fig. 5.* $I_{LD}/(I_{LD} - I_D)$ against $\omega^{1/2}$ plots in (a) oxygen saturated supporting electrolyte at pc platinum; (b) oxygen saturated + 1 mM hydrogen peroxide supporting electrolyte at pc platinum; (c) oxygen saturated supporting electrolyte at tin UPD platinum ($\theta_{Sn} = 0.48$). $T =$ 25 °C. Key: (■—■) 0.60, (●—●) 0.62, (▲—▲) 0.64, (▼—▼) 0.66, (◆—◆) 0.68, (□—□) 0.80, (○—○) 0.82, (△—△) 0.84, (∇—∇) 0.86, (◇—◇) 0.88 V.

Besides, $\bar{k}_2$ values are 10 times higher than those for OERR at bare platinum, indicating a larger proportion of hydrogen peroxide in solution. Moreover, $\bar{k}_3$ values are similar to those found for bare platinum, showing that the formation of hydrogen peroxide is not consumed by a further electroreduction to water.

Table 1 also shows OERR rate constants in hydrogen peroxide supporting electrolyte at bare platinum. These values were calculated for $E_D$ lower than 0.80 V to avoid any hydrogen peroxide oxidation contribution. $\bar{k}_1$ values are 10–15 times smaller than those of $\bar{k}_2$, except at the maximum (0.64 V) where they are nearly the same. Similarly, $\bar{k}_3$ values reach a maximum at 0.50 V but, in general, they are negligible (1000 times smaller than the others). However, $\bar{k}_2$ values decrease monotonously with $E_D$ as a consequence of continuous formation of bulk hydrogen peroxide.

To complete the scheme explanation, the OERR mechanism was analysed from the very first stage of the reaction; that is, the adsorption process. The competition between the different states of adsorbed oxygen on platinum results in a dissociative or a molecular adsorption depending on platinum topology and electrode potential [10, 13, 30–32]. On the one hand, in the case of

*Table 1.* Potential dependence of OERR rate constants in oxygen saturated supporting electrolyte at 25 °C

| Bare pc platinum | | | |
|---|---|---|---|
| $E_D$/V | $\bar{k}_1$/cm$^{-1}$ | $10^2\,\bar{k}_2$/cm$^{-1}$ | $10^4\,\bar{k}_3$/cm$^{-3}$ |
| 0.60 | 0.754 | 0.18 | – |
| 0.62 | 0.348 | 0.84 | – |
| 0.64 | 0.343 | 0.94 | – |
| 0.66 | 0.230 | 1.66 | – |
| 0.68 | 0.190 | 2.63 | 3.6 |
| 0.70 | 0.130 | 5.60 | 4.0 |
| 0.72 | 0.089 | 5.62 | 4.1 |
| 0.74 | 0.048 | 4.74 | 3.5 |
| 0.76 | 0.003 | 2.56 | 2.3 |
| 0.78 | 0.002 | 1.94 | 1.3 |
| 0.80 | – | 1.47 | 1.5 |
| 0.82 | – | 0.78 | 0.9 |
| 0.84 | – | 1.69 | 0.7 |
| 0.86 | – | 0.43 | 0.4 |
| 0.88 | – | 0.22 | 0.2 |
| 0.90 | – | 0.17 | 0.1 |
| Tin UPD ($\theta_{Sn}$ = 0.48) platinum | | | |
| $E_D$/V | $10^3\,\bar{k}_1$/cm$^{-1}$ | $10\,\bar{k}_2$/cm$^{-1}$ | $10^4\,\bar{k}_3$/cm$^{-3}$ |
| 0.38 | 1.21 | 0.80 | 2.22 |
| 0.36 | 1.37 | 1.24 | 2.25 |
| 0.34 | 7.31 | 1.41 | 2.24 |
| 0.32 | 13.6 | 1.59 | 2.50 |
| 0.30 | 21.4 | 1.91 | 2.73 |
| 0.28 | 10.2 | 2.54 | 2.83 |
| 0.26 | 8.1 | 3.63 | 2.86 |
| 0.24 | 7.0 | 4.57 | 3.06 |
| 0.22 | 5.2 | 5.75 | 3.08 |
| 0.20 | 2.9 | 6.42 | 3.11 |
| 0.18 | 1.2 | 8.83 | 3.54 |
| Bare pc platinum in 1 mM hydrogen peroxide | | | |
| $E_D$/V | $10\,\bar{k}_1$/cm$^{-1}$ | $10\,\bar{k}_2$/cm$^{-1}$ | $10^4\,\bar{k}_3$/cm$^{-1}$ |
| 0.44 | 0.153 | 8.95 | 0.23 |
| 0.46 | 0.179 | 7.03 | 1.56 |
| 0.48 | 0.209 | 5.45 | 2.55 |
| 0.50 | 0.235 | 4.26 | 3.21 |
| 0.55 | 0.354 | 3.88 | 2.09 |
| 0.60 | 0.765 | 2.85 | 2.01 |
| 0.62 | 2.30 | 2.68 | 1.78 |
| 0.64 | 5.88 | 2.50 | 1.56 |
| 0.66 | 1.24 | 2.07 | 1.35 |
| 0.68 | 0.743 | 1.44 | 1.12 |
| 0.70 | 0.598 | 1.38 | 0.99 |
| 0.72 | 0.224 | 1.14 | 0.75 |
| 0.74 | 0.131 | 1.05 | 0.66 |
| 0.76 | 0.09 | 0.83 | – |
| 0.78 | 0.07 | 0.67 | – |
| 0.80 | 0.03 | 0.56 | – |

bare platinum, a dissociative adsorption was verified [12, 13] so the following reaction can be postulated;

$$O_2 + 2\,H^+ + 2\,e^- + 2\,Pt \underset{k_{-a}}{\overset{k_a}{\rightleftharpoons}} 2[Pt - OH]_{ad} \qquad (II)$$

On the other hand, in the presence of hydrogen peroxide, $p = 1$ was demonstrated so the formation of peroxide intermediates can be accepted;

$$O_2 + H^+ + e^- + Pt \underset{k_{-b}}{\overset{k_b}{\rightleftharpoons}} [HO - O - Pt]_{ad} \qquad (III)$$

Finally, at tin UPD platinum, $p = 1$ was also obtained indicating the existence of a similar intermediate compound;

$$O_2 + H^+ + e^- + Pt - Pt - Sn \underset{k_{-c}}{\overset{k_c}{\rightleftharpoons}} \left[Pt < \begin{matrix} O-O-H \\ Sn-Pt \end{matrix}\right]_{ad} \qquad (IV)$$

## 5. Conclusions

(i) Tin UPD process was studied on pc platinum by controlling tin(II) solution concentration, deposition time, and applied potential. Potentiodynamic cycling in the 0.05–0.60 V range produces a surface rearrangement of tin adatoms to (1 1 0) sites and hydrogen adatoms to (1 0 0) sites. The maximum surface coverage by tin is 2/3 at UPD levels.

(ii) Rotating ring-disc electrode data for OERR shows bulk hydrogen peroxide formation at tin UPD platinum without peroxide intermediates.

(iii) The reaction order with respect to oxygen varies with the nature of the surface; it is greater than 1 in the case of tin UPD platinum.

(iv) The interpretation of rotating ring-disc data, based on Damjanović's scheme and the analysis of rate constants, leads us to conclude that OERR at tin UPD platinum occurs by the formation of bulk hydrogen peroxide and water as products.

## Acknowledgements

The authors acknowledge the Programa para el Desarrollo de las Ciencias Básicas (PEDECIBA) Química for financial support (Uruguay). C.F.Z. is a researcher at PEDECIBA. G.O. has a fellowship granted by PEDECIBA.

## References

1. E. Yeager, *Electrochim. Acta* **29** (1984) 1527.
2. K.L. Hsueh, E.R. González and S. Srinivasan, *Electrochim. Acta* **28** (1983) 691.
3. A.J. Appleby and S. Baker, *J. Electrochem. Soc.* **125** (1978) 404.
4. P.N. Ross and P.C. Andriacos, *J. Electroanal. Chem.* **154** (1983) 205.
5. R.R. Adzic, *in* R.E. White, J.O'M. Bockris and B.E. Conway (Eds), 'Modern Aspects of Electrochemistry', Vol. 21 (Plenum Press, New York, 1990), chap. 5 pp. 163–235.
6. D.M. Kolb, *in* H. Gerisher and C.W. Tobias (Eds), 'Advances in Electrochemistry and Electrochemical Engineering', Vol. 11 (Interscience, New York, 1978) p. 125.
7. M.W. Breiter, *J. Electrochem. Soc.* **114** (1967) 1125.
8. D. Margheritis, R.C. Salvarezza, M.C. Giordano and A.J. Arvia, *J. Electroanal. Chem.* **229** (1987) 327.

9. S.A.S. Machado, A.A. Tanaka and E.R. González, *Electrochim. Acta* **36** (1991) 1325.
10. C.F. Zinola, A.M. Castro Luna, W.E. Triaca and A.J. Arvia, *Electrochim. Acta*, special issue dedicated to 'Progress in Electrocatalysis: Theory and Practice', **39** (1994) 1627.
11. C.F. Zinola, W.E. Triaca and A.J. Arvia, *J. Appl. Electrochem.* **25** (1995) 740.
12. A Damjanovic and V. Brusic, *Electrochim. Acta* **12** (1967) 615.
13. H. Wroblowa, M.L.B. Rao, A. Damjanovic and J.O'M. Bockris, *J. Electroanal. Chem.* **15** (1967) 139.
14. H. Kita, H. Lei and Y. Gao, *J. Electroanal. Chem.* **379** (1994) 407.
15. M. Drogowska, H. Menard and L. Brossard, *J. Appl. Electrochem.* **21** (1991) 84.
16. X.H. Xia, *Electrochim. Acta* **45** (1999) 1057.
17. A.S. Lapa, *Deposited Doc.* (1981) 575–582.
18. M.O. Argüeso Mengod, Doctoral thesis 'Electrodo de Platino Modificado por Adatomos de Estaño, Cobre y Plomo. Influencia de la Electrooxidación de n-propanol en ácido sulfúrico' (Universidad de São Paulo, 1993).
19. P. Berenz, S. Tillmann, H. Massong and H. Baltruschat, *Electrochim. Acta* **43** (1998) 3035.
20. H. Massong, S. Tillmann, T. Langkau, E.A. Abd El Meguid and H. Baltruschat, *Electrochim. Acta* **44** (1998) 1379.
21. B.J. Bowles, *Nature* **212** (1996) 1456.
22. B.J. Bowles and T.E. Cranshaw, *Phys. Lett.* **17** (1965) 258.
23. S.H. Cadle and S. Brückenstein, *Anal. Chem.* **43** (1971) 932.
24. N. Furuya and S. Motto, *J. Electroanal. Chem.* **72** (1976) 165.
25. H. Angerstein-Kozlowska, *in* E.B. Yeager, J.O'M. Bocris, B.E. Conway and S. Sarangapani (Eds) 'A Comprehensive Treatise of Electrochemistry', Vol. 9 (Plenum Press, New York, 1984), chap. 2, p. 15.
26. C.F. Zinola, J. Tróccoli and J. Rodríguez, in preparation.
27. A. Damjanovic, M.A. Genshaw and J.O'M. Bockris, *J. Chem. Phys.* **45** (1964) 4057.
28. Su-Moon Park, S. Ho, S. Aruliah, M. Weber, C. Ward, R. Venter and S. Srinivasan, *J. Electrochem. Soc.* **113** (1986) 1641.
29. J.D.E. Mc. Intyre and W.F. Peck Jr., 'Chemistry and Physics of Electrocatalysis,' Vol. 84-12, (1984), pp. 102–130.
30. C.F. Zinola, A.M. Castro Luna, W.E. Triaca and A.J. Arvia, *J. Appl. Electrochem.* **24** (1994) 531.
31. A.J. Appleby, *J. Electroanal. Chem.* **357** (1993) 117.
32. F. El Kadiri, R. Faure and R. Durand, *J. Electroanal. Chem.* **301** (1991) 177.